

We are IntechOpen, the world's leading publisher of Open Access books Built by scientists, for scientists

6,900

Open access books available

186,000

International authors and editors

200M

Downloads

Our authors are among the

154

Countries delivered to

TOP 1%

most cited scientists

12.2%

Contributors from top 500 universities



WEB OF SCIENCE™

Selection of our books indexed in the Book Citation Index
in Web of Science™ Core Collection (BKCI)

Interested in publishing with us?
Contact book.department@intechopen.com

Numbers displayed above are based on latest data collected.
For more information visit www.intechopen.com



Atomic Layer Deposition of High-k Oxides on Graphene

Harry Alles, Jaan Aarik, Jekaterina Kozlova,
Ahti Niilisk, Raul Rammula and Väino Sammelselg
*University of Tartu
Estonia*

1. Introduction

Graphene that is a single hexagonal layer of carbon atoms with very high intrinsic charge carrier mobility (more than 200 000 cm²/Vs at 4.2 K for suspended samples; Bolotin, et al., 2008) attracts attention as a promising material for future nanoelectronics. During last few years, significant advancement has been made in preparation of large-area graphene. The lateral sizes of substrates for graphene layers have been increased up to $\frac{3}{4}$ m (Bae et al., 2010) and continuous roll-to-roll deposition of graphene has been published (Hesjedal, 2011). This kind of progress might allow one to apply similar planar technologies for fabricating graphene-based devices in future as currently used for processing of silicon-based structures.

After very first experiments (Novoselov et al., 2004), in which the electrical properties of isolated graphene sheets were characterized, a lot of attention has been paid to the similar studies, i.e. investigation of uncovered graphene flakes deposited on oxidized silicon wafers that served as back gates. However, in order to realize graphene-based devices, a high-quality dielectric on top of graphene is required for electrostatic gates as well as for tunnel barriers for spin injection. For efficient control of charge carrier movement dielectric layers deposited on graphene should be very thin, a few nanometers thick, and of very uniform thickness without any pinholes. At the same time, the dielectric should possess high dielectric constant, high breakdown voltage and low leakage current even at a small thickness. And, of course, it is expected that the high mobility of charge carriers in graphene should not be markedly affected by the dielectric layer.

In order to make top-gated graphene-based Field Effect Transistor (FET), Lemme et al. (2007) applied evaporation techniques for preparation of a gate stack with ~20 nm thick SiO₂ dielectric layer on graphene. They used p-type Si(100) wafers with a boron doping concentration of 10¹⁵ cm⁻³, which were oxidized to a SiO₂ thickness of 300 nm. On these wafers, micromechanically exfoliated graphene flakes were stucked. The Ti/Au source and drain electrodes were prepared using optical lift-off lithography. Next, electron beam lift-off lithography was applied to define a top gate electrode on top of the graphene flake covered with the dielectric (Fig. 1a).

Lemme et al. were first to demonstrate that the combined effect of back and top gates can be applied to graphene devices. However, measurements of the back-gate characteristics before

and after the evaporation of the top gate revealed that deposition of the dielectric layer caused a considerable decrease in the drain current of the device (Fig. 1b). In addition, the current modulation through the back gate was reduced by the top gate. After this degradation the room-temperature electron and hole mobilities in graphene were as low as $710 \text{ cm}^2/\text{Vs}$ for holes and $530 \text{ cm}^2/\text{Vs}$ for electrons, i.e. comparable to the typical charge carrier mobilities in silicon.

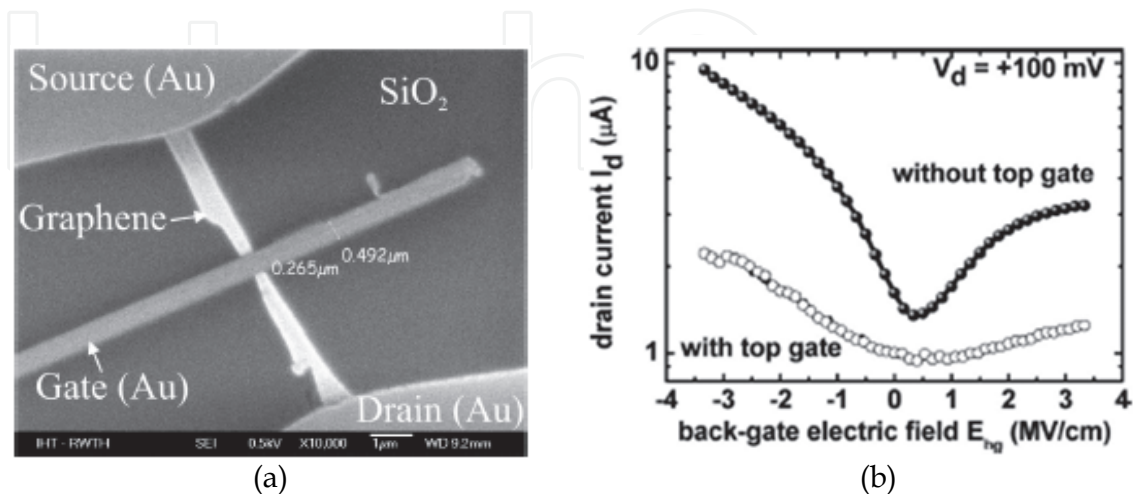


Fig. 1. (a) Scanning Electron Microscope image of a graphene FET. (b) Back-gate transfer characteristics of the graphene FET with and without a top gate (Adapted from Lemme et al., 2007).

Using Raman spectroscopy, Ni et al. (2008a) have studied the effect of deposition of different dielectrics with various methods on top of graphene sheets. Figure 2 presents Raman spectra after deposition of SiO_2 layer by Electron Beam Evaporation (EBE), Pulsed Laser Deposition (PLD) and Radio Frequency (RF) sputtering methods, HfO_2 layer by PLD and polymethyl methacrylate (PMMA) layer by spin coating on top of graphene. As it can be seen, the used deposition methods (with the exception of spin coating) caused defects which showed up as appearance of the D-band in Raman spectra ($\sim 1350 \text{ cm}^{-1}$) of graphene.

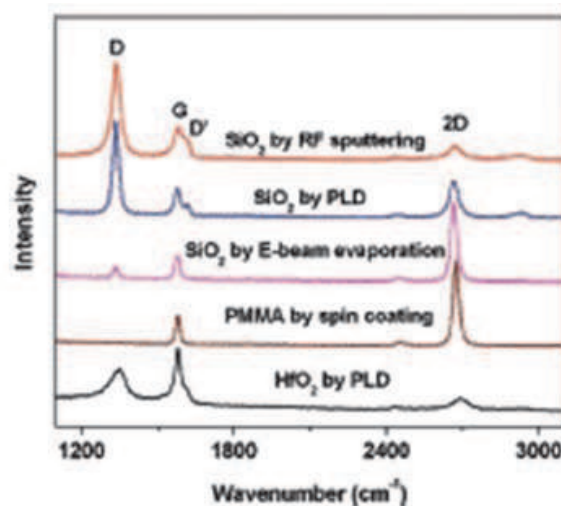


Fig. 2. Raman spectra of graphene after deposition of SiO_2 by RF sputtering, PLD and EBE, PMMA by spin coating and HfO_2 by PLD. (Adapted from Ni et al., 2008a).

On the basis of the Raman spectra, one can conclude that electron-beam evaporation and, particularly, sputtering and PLD processes may cause significant damages to graphene. Due to that influence the mobility values of the top-gated graphene-based devices prepared using these methods are typically by an order of magnitude smaller than those of back-gated devices (Lemme et al., 2007). For this reason, alternative methods for deposition of dielectrics on graphene have been extensively investigated.

In the case of traditional nanoelectronic devices, a very suitable method for controlled deposition of ultrathin homogeneous films is Atomic Layer Deposition (ALD). However, ALD of thin films on graphene is not easy because there are no dangling bonds on the defect-free graphene surface, which are needed for chemical surface reactions the conventional ALD processes are based on. Nevertheless, several groups have been able, using ALD technique, to deposit thin and continuous HfO_2 layers on pristine as-cleaved graphene (Meric et al., 2008; Zou et al., 2010; Alles et al., 2011). It has also been reported that after ALD of relatively thin Al_2O_3 layers directly on graphene (Moon et al., 2009; Nayfeh, 2011), top-gated devices with good performance can be obtained.

In order to better nucleate the growth of dielectric on graphene and obtain smooth uniform films, the graphene surface has been pretreated prior ALD (Williams et al., 2007), e.g. by using recipes successfully tested on carbon nanotubes (Farmer & Gordon, 2006). Later, other approaches for pretreatment of graphene surface have been applied as well. For instance, a thin (~1 nm thick) metal seed layer of Al that was oxidized before ALD (Kim et al., 2009) or polymer films (Wang et al., 2008; Farmer et al., 2009; Meric et al., 2011) have been deposited on graphene in order to initiate ALD of high-k dielectrics. In addition, pretreatment of the graphene surface with ozone prior ALD of Al_2O_3 has been investigated (Lee et al., 2008, 2010).

In this work, we compare ALD experiments in which graphene has been covered by high-k dielectrics (Al_2O_3 and HfO_2) either directly or after surface functionalization. Particular attention is focussed on attempts to grow dielectric films with higher density (and dielectric constant) using higher substrate temperatures and two-temperature ALD processes that start with formation of a thin seed layer at low temperature and proceed with depositing the rest of the dielectric layer at high temperature.

2. ALD of high-k dielectrics directly on graphene

2.1 ALD of amorphous Al_2O_3 and HfO_2 directly on graphene

Wang et al. (2008) have tried to deposit a thin Al_2O_3 layer, ~2 nm thick, on mechanically exfoliated graphene sheets, which were carefully cleaned by annealing at 600 °C in Ar atmosphere at a pressure of 1 Torr. The deposition of Al_2O_3 on graphene at 100 °C using vapors of trimethylaluminum (TMA; $\text{Al}(\text{CH}_3)_3$) and water (H_2O) as precursors was unsuccessful – the Al_2O_3 film was preferentially formed on graphene edges and defect sites. On the basis of these results, it was concluded that ALD of metal oxides gives no direct deposition on defect-free pristine graphene.

Similar results were obtained by Xuan et al. (2008) who tried to deposit Al_2O_3 and HfO_2 films on Highly Ordered Pyrolytic Graphite (HOPG) surfaces. Fresh HOPG surfaces, obtained using Scotch tape, were transferred into ALD reactor immediately after cleaving and 1-35 nm thick Al_2O_3 films were deposited at the temperature of 200–300 °C by alternating pulses of TMA and H_2O as precursors. For ALD of HfO_2 , HfCl_4 and H_2O were used as precursors. As a result, Xuan et al. obtained large number of Al_2O_3 and HfO_2

nanoribbons, with dimensions of 5 - 200 nm in width and more than 50 μm in length. This was due to the existence of numerous step edges on HOPG surfaces, which served as nucleation centers for the ALD process.

In our ALD experiments, we deposited thin Al_2O_3 film directly onto exfoliated graphene using AlCl_3 - H_2O precursor combination. During the film growth, the precursor pulses and N_2 purge period after the AlCl_3 pulse were 2 seconds while the N_2 purge period after the H_2O pulse was 5 seconds in duration. To initiate nucleation, 4 cycles were applied at a substrate temperature of 80 $^\circ\text{C}$. Then the temperature was increased to 300 $^\circ\text{C}$ and 50 cycles were applied. It was found, however, that such a deposition process still provided non-uniform coverage with large number of pinholes (Fig. 3a). About 4 nm thick Al_2O_3 film on graphene had the rms surface roughness value of ~ 1.6 nm while the roughness value of the film on SiO_2 was only 0.45 nm. Atomic Force Microscope (AFM) measurements revealed that some of the pinholes penetrated through the whole film. These results clearly correspond to the previous reports (Wang et al., 2008; Xuan et al., 2008) and indicate that Al_2O_3 nucleation directly onto graphene is retarded due to the absence of favourable surface sites. At the same time the Raman spectra of the same sample, presented in Fig. 3b, reveal that the ALD process has not generated defects in graphene. However, blueshifts of G- and 2D-bands indicate that the deposition process and/or deposited film influenced properties of graphene. Possible reasons for this influence will be discussed in Sec. 2.2.

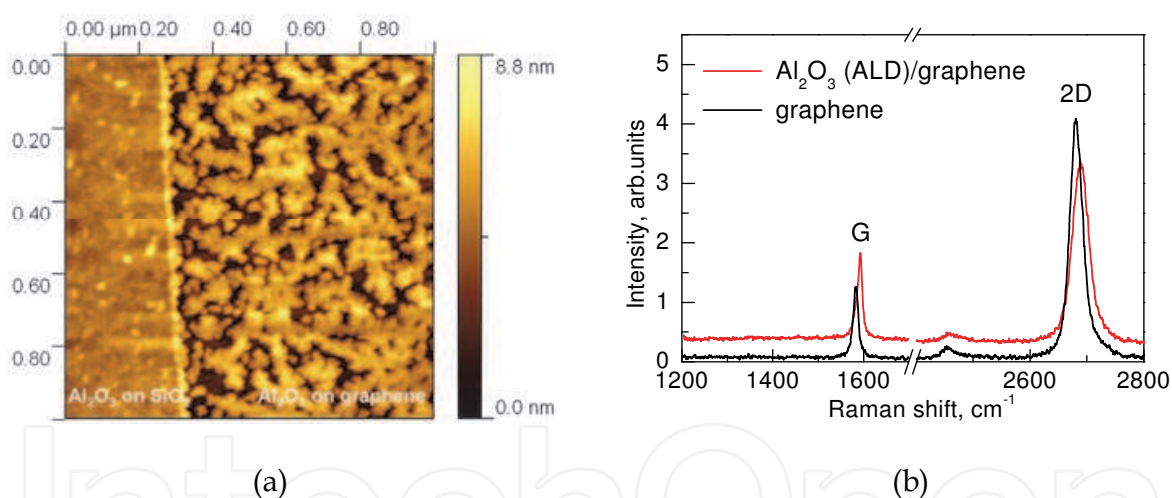


Fig. 3. (a) AFM image ($1 \times 1 \mu\text{m}^2$) of a single layer graphene flake (right) on SiO_2 , both surfaces covered with ~ 4 nm thick Al_2O_3 layer and (b) typical Raman spectra from the same graphene flake before and after the ALD of Al_2O_3 .

Very recently Nayfeh et al. (2011) reported about successful remote plasma-assisted ALD experiments in which Al_2O_3 gate dielectric was directly deposited onto chemical-vapor-deposited (CVD) monolayer graphene at 100 $^\circ\text{C}$. They used 100 cycles consisting of TMA exposure for 0.06 s, purge for 30 s, oxygen (20 sccm) plasma exposure for 1 s and purge for 45 s. *In situ* annealing at 250 $^\circ\text{C}$ was also performed to improve Al_2O_3 film quality. AFM and Raman measurements showed a uniform dielectric coverage of graphene together with a slight increase in the disorder and signs of additional doping (see Fig. 4). This deposition process has enabled the fabrication of graphene FETs with ~ 9 nm thick gate insulator, which had a peak field-effect mobility of 720 cm^2/Vs for holes.

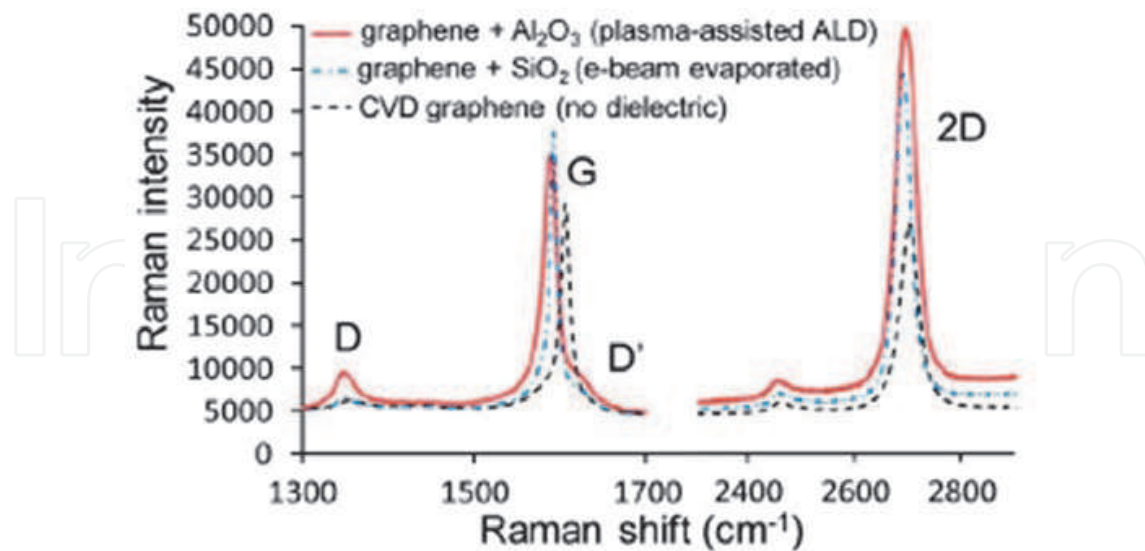


Fig. 4. Raman measurements of a CVD graphene before dielectric deposition and after 100 cycles of plasma-assisted ALD of Al_2O_3 , and for a comparison, also after EBE of 9 nm SiO_2 . (Adapted from Nayfeh et al., 2011).

A few years ago, Meric et al. (2008) reported about their experiments on ALD of 5-15 nm thick HfO_2 films on exfoliated graphene. They used tetrakis(dimethylamino)hafnium(IV) ($\text{Hf}(\text{NMe}_2)_4$) and water (H_2O) as the precursors and the deposition temperature was 90°C . The pulse time for hafnium precursor was 0.3 s, which was followed by a 50 s purge, 0.03 s H_2O pulse and 150 s purge. The resulting growth rate was about 0.1 nm/cycle and the dielectric constant of the HfO_2 film obtained was ~ 16 as determined by C-V measurements.

Figure 5a shows an AFM image of a single layer graphene flake on SiO_2 coated with a 5 nm thick HfO_2 layer grown immediately after mechanical exfoliation. As the measured height difference over the edge of the graphene is approximately the same (~ 0.9 nm) as before the ALD of HfO_2 layer, one can conclude that the growth has taken place at the same rate on the SiO_2 and graphene surfaces. Meric et al. suggested that the growth was most likely due to physisorption, enhanced by the low-temperature growth procedure.

Meric et al. observed, however, that the roughness of the oxide on top of graphene was noticeably, by about 30%, higher than on the surrounding SiO_2 . This result demonstrates that even at this very low temperature, uniformity of adsorption of precursors is not sufficient on graphene. Meric et al. also found that the mobility of the graphene sheet is almost the same before and after HfO_2 growth (Fig. 5b).

Recently, using the same precursors, pinhole-free 10 nm thick amorphous HfO_2 films have been deposited on exfoliated graphene at a temperature of 110°C by Zou et al. (2010) who achieved the low-temperature mobility of charge carriers as high as $\sim 20\,000\text{ cm}^2/\text{Vs}$ in HfO_2 -covered graphene. To identify the growth mechanism, they have studied the deposition of HfO_2 films with various thicknesses on single- and multi-layer (5-6 layers) graphene flakes on SiO_2 substrates. On single-layer graphene flakes, they achieved the coverage of about 98% when depositing 2.5 nm thick HfO_2 films. Films thicker than 10 nm were pinhole-free and showed excellent morphology with the rms surface roughness of 0.2-0.3 nm, comparable to that of the HfO_2 film deposited on the SiO_2 substrate.

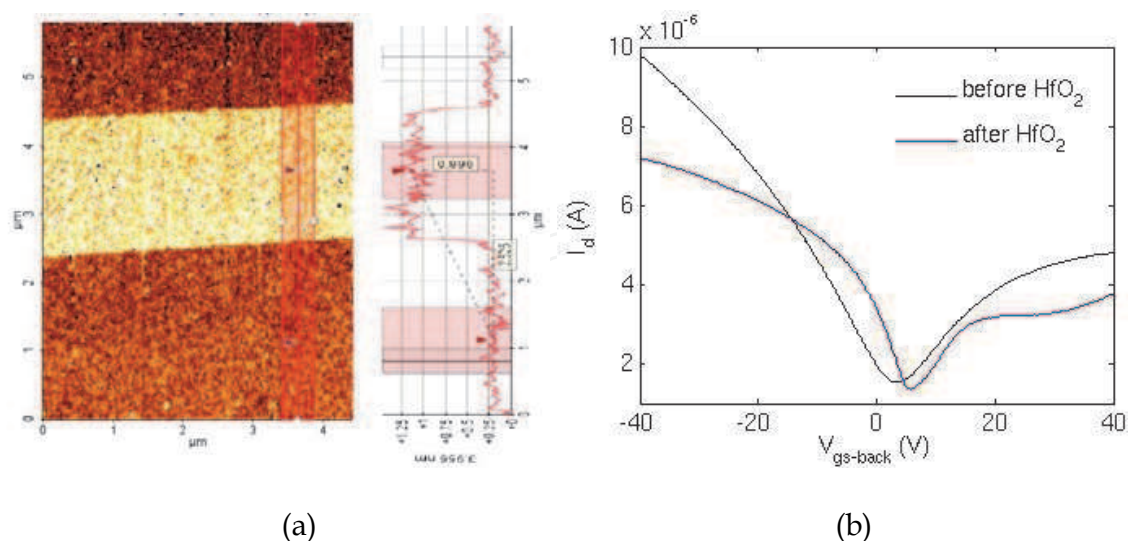


Fig. 5. (a) AFM image and profile of a graphene flake covered with 5 nm HfO_2 . (b) Back-gate transfer characteristics of the graphene-based FET (the gate width is $1.5 \mu\text{m}$ and the length is $3 \mu\text{m}$) before and after the deposition of HfO_2 . (Adapted from Meric et al., 2008).

On the other hand, HfO_2 films deposited on thicker graphene flakes exhibited much poorer quality as the coverage of 2.5 nm thick HfO_2 films on 5-6 layer graphene was only about 50% and pinholes remained even in 20 nm thick HfO_2 films. Zou et al. also found that the surfaces of single-layer graphene flakes were significantly rougher than those of multi-layer flakes. According to their explanation, the curvature existing in single-layer graphene flakes facilitates adsorption of the precursors. This explanation is in agreement with the observations of other groups who have recorded low coverage of the oxide layers on clean HOPG surfaces (Xuan et al., 2008).

2.2 ALD of crystalline HfO_2 films on as-cleaved graphene

The ALD processes described in the previous section have been performed at relatively low substrate temperatures. The films deposited at these temperatures are amorphous and for this reason possess relatively low dielectric constant. In order to obtain higher dielectric constant values, higher substrate temperatures yielding films with higher purity and density are required during the deposition of dielectrics. In our recent study (Alles et al., 2011), we have deposited HfO_2 films directly on as-cleaved graphene from HfCl_4 and H_2O using three different processing regimes with substrate temperatures of (i) 180°C for deposition of the whole dielectric layer, (ii) 170°C for deposition of a 1 nm thick HfO_2 seed layer and 300°C for deposition the rest of the dielectric layer, and (iii) 300°C for deposition of the whole dielectric layer. An ALD cycle consisted of an HfCl_4 pulse (5 s in duration), purge of the reaction zone with N_2 (2 s), H_2O pulse (2 s) and another purge (5 s).

Relatively smooth HfO_2 films were obtained on graphene at the low temperature of 180°C . In the best cases, the rms surface roughness was less than 0.5 nm for ~ 30 nm thick films (see Fig. 6a). This value is comparable to the rms roughness of the same HfO_2 film on SiO_2 , which was the substrate for the graphene flakes. The films were amorphous according to the Raman spectroscopy data (see Fig. 7).

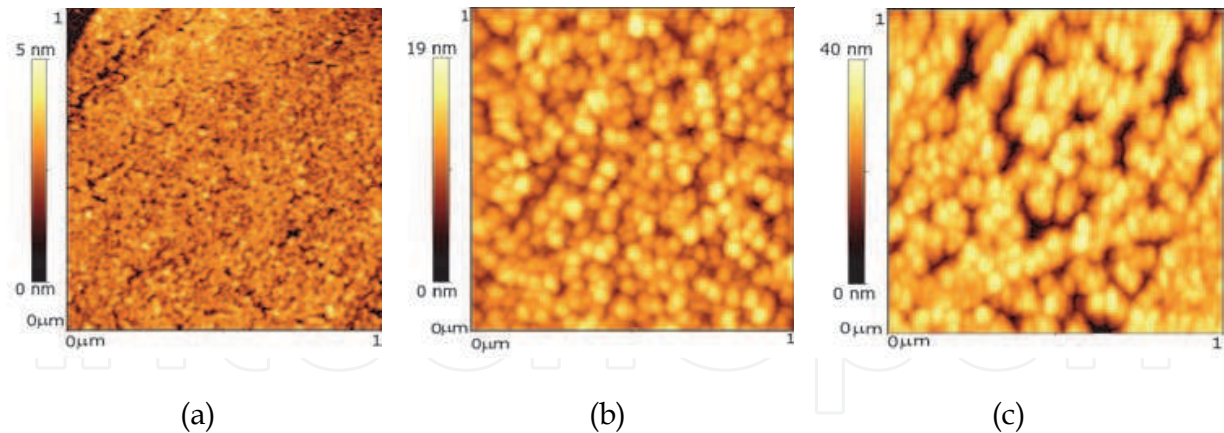


Fig. 6. AFM images of ~ 30 nm thick HfO_2 films on top of graphene flakes deposited at 180°C (the rms surface roughness < 0.5 nm), (b) in a two-temperature ($170/300^\circ\text{C}$) process (the rms surface roughness ~ 2.5 nm) and (c) at 300°C (the rms surface roughness ~ 5 nm).

The HfO_2 films deposited to a thickness of 30 nm in a two-temperature process had the rms surface roughness values of ~ 2.5 nm and ~ 2 nm on graphene and on SiO_2 , respectively (Fig. 6b), and we recorded also Raman scattering from monoclinic HfO_2 (Fig. 7). At the same time, the surface roughness of ~ 30 nm thick HfO_2 films grown at 300°C from the beginning of deposition process was as high as 5 nm on graphene and 2 nm on SiO_2 . Scattering from monoclinic HfO_2 was recorded for these films as well (Fig. 7).

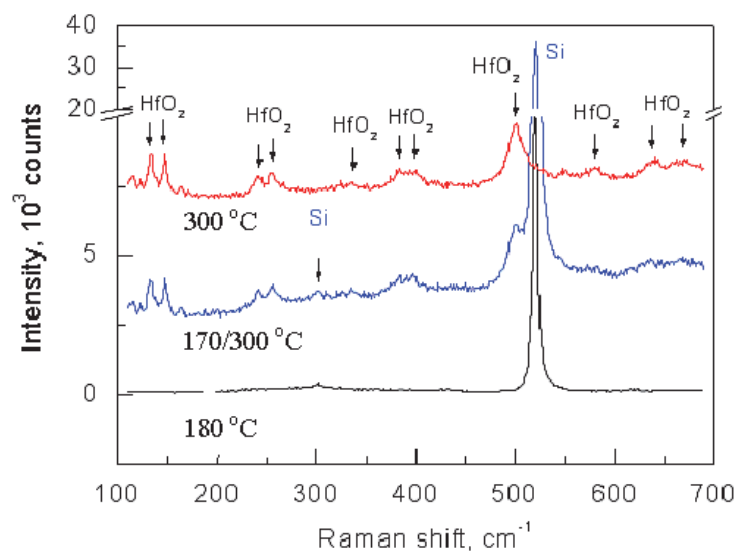


Fig. 7. Raman spectra from HfO_2 films on top of graphitic flakes deposited at 180°C , $170/300^\circ\text{C}$ and 300°C .

In our study, we found that the rms surface roughness of ~ 10 nm thick HfO_2 films grown on graphene was markedly lower (~ 1.7 nm) compared with that of ~ 30 nm thick HfO_2 films (~ 2.5 nm). Similar difference in surface roughness was observed for films deposited on SiO_2 . Thus, the rougher surface of thicker HfO_2 films is due to crystallization of HfO_2 during the film growth at higher temperature rather than because of nucleation problems on the surface of graphene.

At the edge of a single layer graphene flake, the AFM surface profile of the HfO_2 film deposited in the two-temperature process (see Fig. 8) corresponded very well to the profile recorded before deposition of the dielectric. This means that HfO_2 film grew at the same rate on graphene and SiO_2 . However, as the surface of HfO_2 films is still somewhat rougher on graphene compared to that on SiO_2 , the parameters of ALD process and the thickness of the seed layer need further optimization.

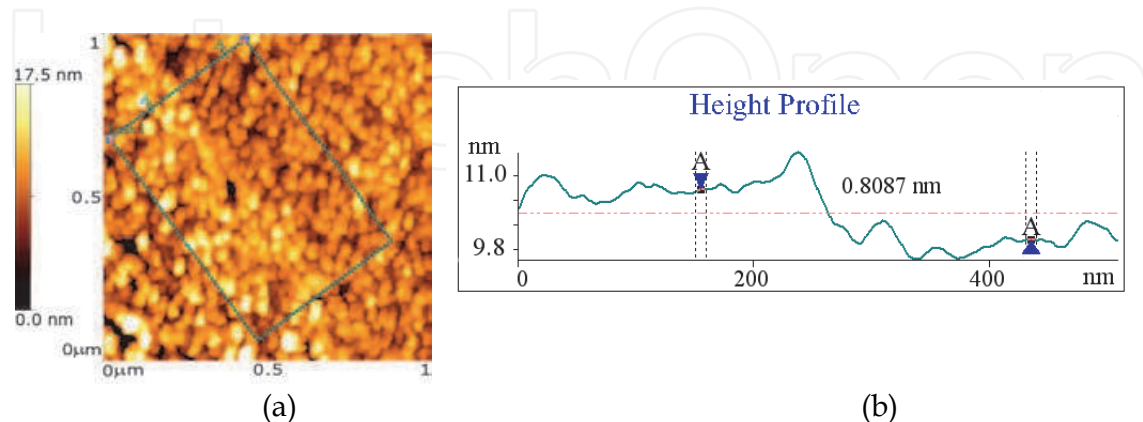


Fig. 8. (a) AFM image of an edge of a single layer graphene flake after deposition of an 11 nm thick HfO_2 layer in a two-temperature process (the rms surface roughness is 1.7 nm on graphene and 0.9 nm on SiO_2). (b) AFM height profile over the edge shown in (a). (Adapted from Alles et al., 2011).

Figure 9 shows the Raman spectra of a single layer graphene flake taken at the same location before and after the deposition of an 11 nm thick HfO_2 layer in a two-temperature process. The intensities of peaks are lower after deposition and the background level has increased. But most importantly, the spectra reveal that noticeable blueshifts of G- (at $\sim 1580 \text{ cm}^{-1}$) and 2D-bands ($\sim 2670 \text{ cm}^{-1}$) of graphene by 9 cm^{-1} and 22 cm^{-1} , respectively, have appeared as a result of HfO_2 deposition.

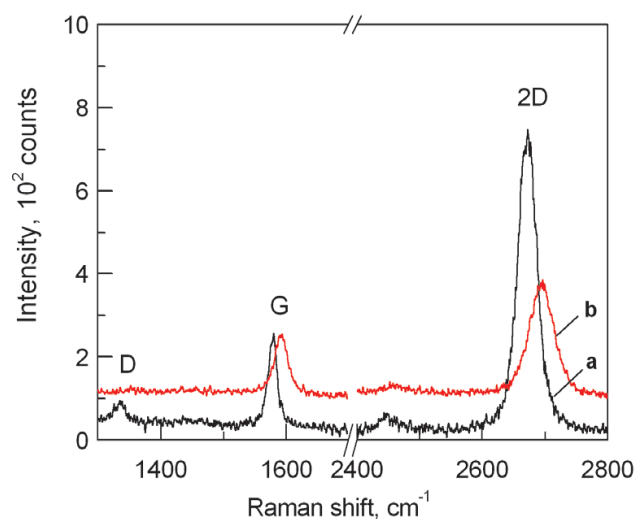


Fig. 9. Raman spectra of a single-layer graphene flake taken at the same point (a) before and (b) after the deposition of an 11 nm thick HfO_2 layer in a two-temperature ($170/300 \text{ }^\circ\text{C}$) process. (Adapted from Alles et al., 2011).

It is known that doping of graphene can influence the positions of Raman peaks (Das et al., 2008; Ni et al., 2008b) but the shift of the 2D-band in this case cannot be greater than that of G-band. In our experiments, however, the shift of the 2D-band is markedly greater. Edge effects and/or changes in the doping level can also cause changes in the peak positions but in that case narrowing of the G-peak should take place (Casiraghi et al., 2007; Ni et al., 2008b). In our case, on the contrary, the width of the G-peak increases. We also performed annealing experiments with a single layer graphene flake under conditions similar to those used during two-temperature ALD process of HfO₂. We observed blueshifts of G- and 2D-peaks by 4 cm⁻¹ and 7 cm⁻¹, respectively. At the same time full width at half maximum (FWHM) of the 2D-peak slightly increased by a few cm⁻¹, while FWHM of the G-peak decreased by ~4 cm⁻¹. On the basis of these data, doping of graphene, edge effects, and influence of high-temperature treatment during the ALD process could be excluded from the list of most important reasons for changes of Raman spectra caused by deposition of HfO₂.

Thus, the compressive strain developed in graphene during the two-temperature ALD process is the most probable reason for the blueshifts in the Raman spectra. Using the biaxial strain coefficient of -58 cm⁻¹/ % for the Raman G-mode and -144 cm⁻¹/ % for the Raman 2D-mode (Mohiuddin et al., 2009) and assuming elastic behavior of graphene, we estimated the compressive strain to be ~0.15% in our single layer graphene flake. This strain can be well explained by the relatively large and negative thermal expansion coefficient of graphene ($7 \times 10^{-6} \text{ K}^{-1}$ at room temperature; Bao et al., 2009) while the thermal expansion of HfO₂ is of the same magnitude but with opposite (positive) sign (Wang et al., 1992), and it indicates strong adhesion of HfO₂ to graphene.

3. ALD of high-k dielectrics on functionalized graphene

3.1 ALD of Al₂O₃ on graphene after treatment with NO₂ and TMA

In order to reduce the leakage currents through the Al₂O₃ gate dielectric deposited on graphene, Williams et al. (2007) adopted the method proposed by Farmer & Gordon (2006) for pretreatment of carbon nanotubes and used NO₂ and TMA for functionalization of the graphene surface prior ALD of Al₂O₃. The exfoliated graphene flakes were cleaned with acetone and isopropyl alcohol (IPA) immediately before inserting them into the ALD reactor. Next, after the chamber was pumped down to a pressure of 0.3 Torr, non-covalent functionalization layer (NCFL) was deposited at room temperature using 50 cycles of NO₂ and TMA followed by 5 cycles of H₂O-TMA in order to prevent desorption of the NCFL. Finally, Al₂O₃ was grown at 225 °C with 300 ALD cycles, each of those consisting of a pulse of H₂O vapor (1 Torr, 0.2 s) and a pulse of TMA vapor (1.5 Torr, 0.1 s), under continuous flow of N₂ and with 5 s intervals between pulses. As a result, ~30 nm thick oxide layer was obtained on top of graphene consisting of NCFL and Al₂O₃ and having a mean dielectric constant $k \sim 6$.

The same recipe was later also used by Lin et al. (2009), who fabricated top-gated graphene-based FETs operating at gigahertz frequencies (up to 26 GHz). They functionalized the surface of exfoliated graphene with 50 cycles of NO₂-TMA and deposited after that a 12 nm thick Al₂O₃ layer as the gate insulator. The dielectric constant of the oxide layers was determined by C-V measurements to be ~7.5. However, in their experiments severe degradation of measured mobilities (down to ~400 cm²/Vs) was observed. Consequently, although this kind of functionalization process allows one to deposit thin (of

the order of 10 nm) pinhole-free gate dielectrics on graphene by ALD, this can cause a significant reduction of field-effect mobility of charge carriers and, correspondingly, the channel conductance of graphene-based FETs.

3.2 ALD of Al₂O₃ on graphene after ozone treatment

Lee et al. (2008, 2010) investigated coating of exfoliated graphene and HOPG surfaces with Al₂O₃ layer in O₃-based ALD process. First, they used freshly cleaved HOPG surfaces and found that while TMA-H₂O process caused selective deposition of Al₂O₃ only along step edges (as in the experiments of Xuan et al. (2008)), the TMA/O₃ process began to provide nucleation sites on basal planes of HOPG surface. Lee et al. (2008) proposed that the chemically inert HOPG surface was converted to hydrophilic mainly through epoxide functionalization.

Later, in order to deposit a uniform Al₂O₃ dielectric layer on top of a graphene flake, they used an ALD seed layer (~1 nm in thickness) grown by applying 6 cycles of TMA and O₃ at 25 °C. After that 155 cycles of TMA/H₂O at 200 °C were applied to deposit additional Al₂O₃ layer (~15 nm in thickness). For their films, they obtained the dielectric constant $k \sim 8$, which is higher than the value typically reported for the Al₂O₃ films deposited on graphene flakes. The mobilities of their devices reached ~5000 cm²/Vs. Lee et al. (2010) also found out that an O₃ treatment at 25 °C introduces minor amount of defects in a single layer graphene, while a substantial number of defects appear at 200 °C (Fig. 10).

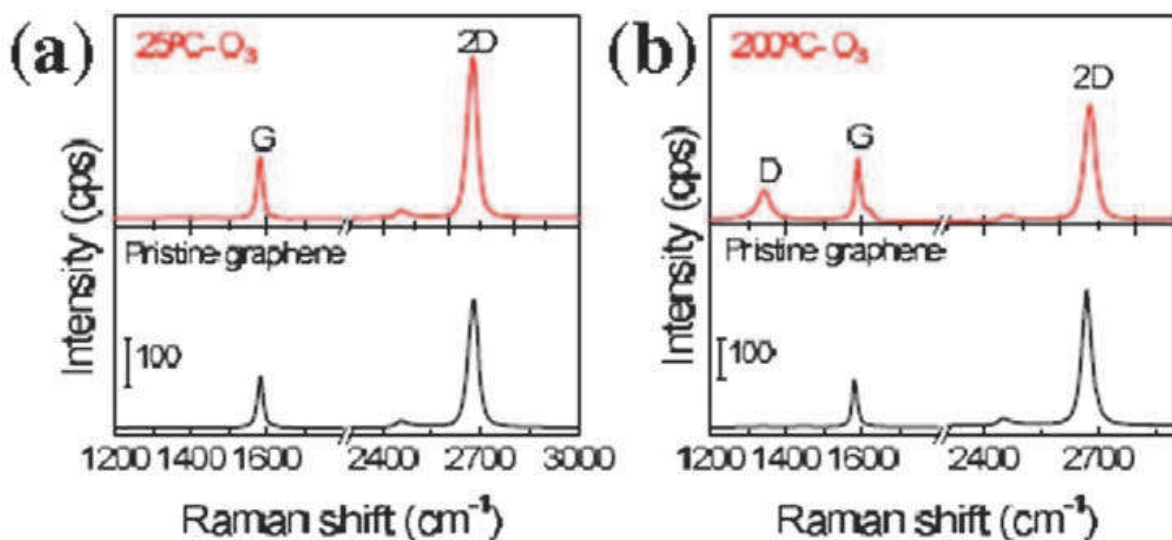


Fig. 10. Raman spectra of a pristine single layer graphene (bottom) and after treatment (top) (a) with O₃ at 25 °C and (b) with O₃ at 200 °C for 20 s. (Adapted from Lee et al., 2010).

3.3 Metal seed layer for ALD of Al₂O₃ on graphene

In order to make graphene-based top-gated FETs, Kim et al. (2009) first annealed the chips with exfoliated graphene flakes in a hydrogen atmosphere at 200 °C and then deposited a thin layer of Al by e-beam evaporation. After oxidization this layer served as a nucleation

layer to enable ALD of Al_2O_3 . TMA and H_2O were used as precursors and 167 cycles resulted in about 15-nm thick Al_2O_3 layer on graphene. The devices fabricated using this technique indicated the mobility in excess of $6000 \text{ cm}^2/\text{Vs}$ at room temperature. Consequently, the top-gate stack did not increase the carrier scattering significantly. A similar approach has later been used by several other groups, also with epitaxial graphene (Robinson, et al., 2010) and CVD graphene (Wu et al., 2011).

3.4 Polymer buffer layer for ALD of Al_2O_3 on graphene

Wang et al. (2008) used a polymer film as a buffer layer in order to cover carefully cleaned graphene with a very thin ($\sim 2\text{-}3 \text{ nm}$) Al_2O_3 layer. They soaked the chip with graphene flakes in 3,4,9,10-perylene tetracarboxylic acid (PTCA) solution for $\sim 30 \text{ min}$, rinsed thoroughly and blew dry. The chip was then immediately moved into the ALD reactor and Al_2O_3 was deposited from TMA and H_2O at 100°C . Figure 11 shows the AFM images of a graphene flake before and after ALD. Uniform coverage with an ultrathin Al_2O_3 film was achieved as the measured rms surface roughness of Al_2O_3 on graphene was as low as 0.33 nm .

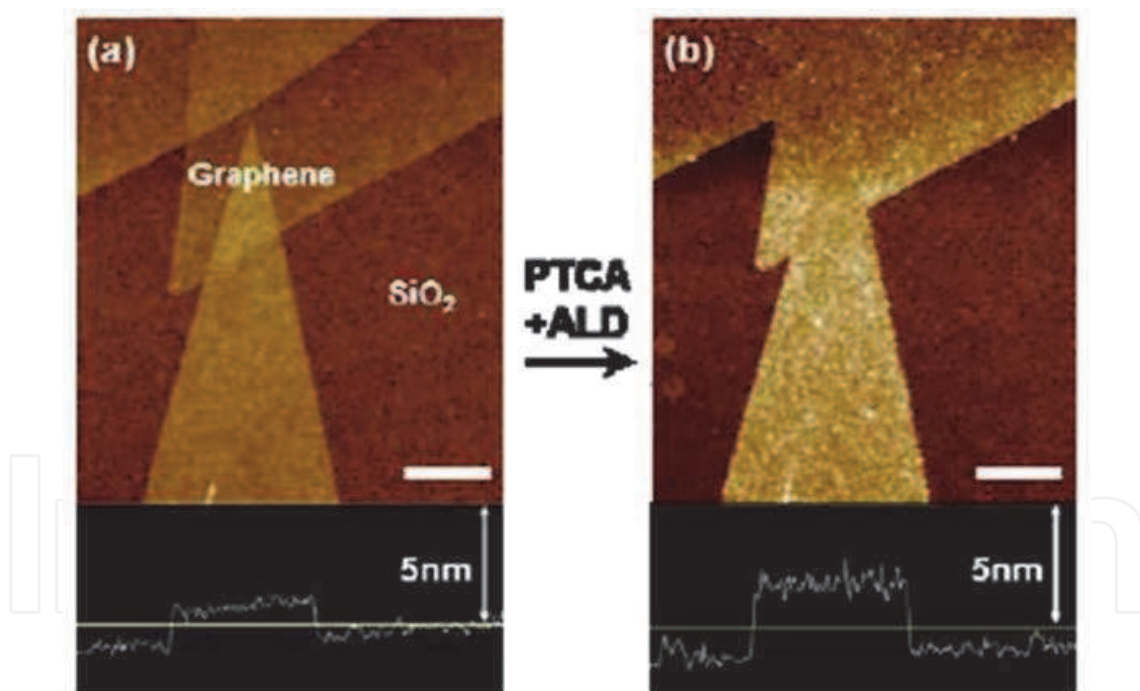


Fig. 11. AFM images of graphene (a) before ALD and (b) of the same area after $\sim 2 \text{ nm}$ Al_2O_3 deposition. Scale bar is 500 nm . (Adapted from Wang et al., 2008).

3.5 Metal seed layers for ALD of HfO_2 on graphene

Fallahazad et al. (2010) have investigated the carrier mobility in a single layer and bilayer exfoliated graphene with a top HfO_2 dielectric as a function of the HfO_2 film thickness and temperature. Prior to the HfO_2 film with ALD technique, a thin ($\sim 1.5 \text{ nm}$) seed layer of Al was deposited by e-beam evaporation. The HfO_2 layer was deposited at 200°C from

Hf(NMe₂)₄ and H₂O as precursors, without any postdeposition annealing. The relative dielectric constant of the stack was found to be about 16. A considerable mobility reduction to about 50% of the initial value was observed after the first 2-4 nm of metal oxide deposition. The mobility did not depend significantly on temperature in the range from 77 K to room temperature. This result suggests that phonon scattering did not play an essential role in the devices. Therefore the authors of this study speculated that influence of positively charged oxygen vacancies, ubiquitous in high-k dielectrics, was the main mobility limiting factor.

3.6 Polymer buffer layer for ALD of HfO₂ on graphene

Farmer et al. (2009) used a low-k polymer (NFC 1400-3CP) as a buffer layer for ALD of HfO₂ on exfoliated graphene. This polymer is a derivative of polyhydroxystyrene that is commonly used in lithography. The polymer can be diluted in propylene glycol monomethyl ether acetate (PGMEA) and spin-coated on top of graphene. For deposition of HfO₂, Farmer et al. used Hf(NMe₂)₄ and H₂O as precursors and carried the ALD process out at 125 °C. The process yielded HfO₂ films with a dielectric constant of about 13 on graphene.

Farmer et al. also found that in order to produce continuous functionalization layer on graphene, a 24:1 dilution (by volume) of PGMEA/NFC is sufficient. Spinning of such a solution at a rate of 4000 rpm for 60 s results in a layer of about 10 nm in thickness. After curing the buffer layer at 175 °C for 5 min to remove residual solvent, a 10-nm thick HfO₂ layer was deposited on top of that. The dielectric constant of the buffer layer was determined to be 2.4 which is a reasonable value for this polymer.

The recipe of Farmer et al. was also used by Lin et al. (2010) who demonstrated cutoff-frequency as high as 100 GHz for top-gated FETs based on wafer-scale epitaxial graphene made from SiC. This cut-off frequency exceeds that of Si metal-oxide semiconductor FETs of the same gate length (~40 GHz at 240 nm). The carrier mobilities were maintained between 900 to 1520 cm²/Vs across the 2-inch wafer. These values were largely the same as before the deposition of a top gate stack.

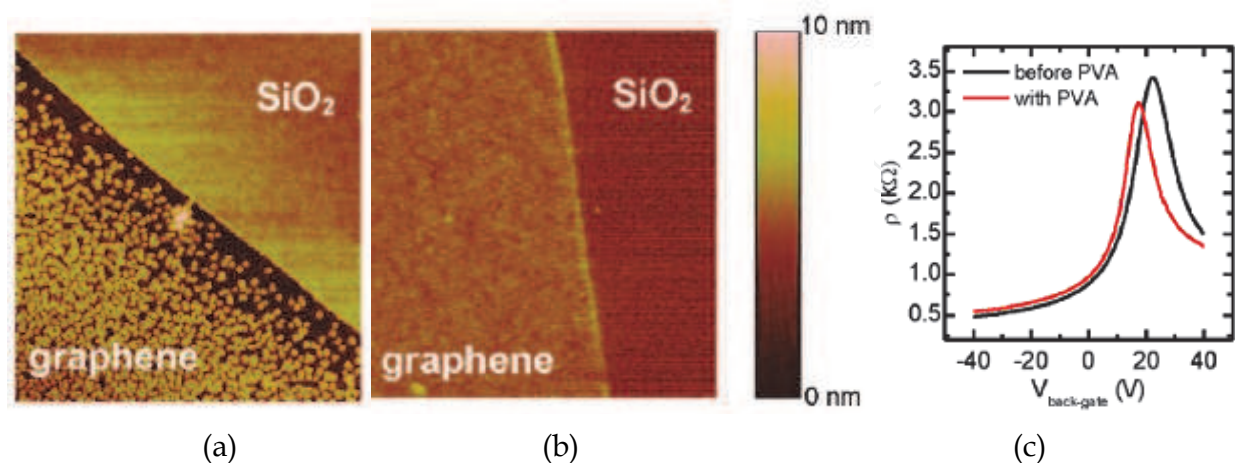


Fig. 12. (a) AFM image over an edge of a graphene flake on SiO₂ after ALD of a 5 nm thick HfO₂ (a) without and (b) with PVA. (c) Resistivity of a device after annealing and the PVA deposition as a function of back-gate bias (Adapted from Meric et al., 2011).

In their later experiments, Meric et al. (2011) have used PVA (poly(vinyl)alcohol) to provide a surface to seed ALD growth on exfoliated graphene. PVA is known to have a relatively high dielectric constant ($k \sim 6$). After the contact deposition they first cleaned the graphene surface by annealing at 330 °C for 3 h in forming gas and then dipped into an 1% aqueous solution of PVA for 12 h. This procedure resulted in ~2.5 nm thick layer of PVA on the graphene surface. After that a brief UV/ozone treatment was employed to activate the -OH groups before the ALD growth of HfO₂ at 150 °C with Hf(NMe₂)₄ and H₂O for 50 cycles, yielding a 5-nm thick HfO₂ film (see Fig. 12b). As a result, the doping and the mobility of the top-gated graphene-based FET stayed relatively unchanged (see Fig. 12c).

Merik et al. (2011) also found that without PVA, ALD growth proceeds only on the SiO₂ area (see Fig. 12a) and the occasional patches of oxide on graphene are formed most likely by surface contamination.

4. Conclusion

As integration of graphene with high-quality ultrathin dielectrics is very important in development of graphene-based nanoelectronic devices, significant efforts have been concentrated on ALD of dielectric films on the graphene surface. An expected result of these studies is that at substrate temperatures most frequently used for ALD, i.e. at 200–400 °C, the deposition of uniform dielectric layers on clean surface of graphene is not possible due to the chemical inertness of this surface. However, using low-temperature ALD, several research groups have succeeded to grow dielectrics (e.g. Al₂O₃ and HfO₂) even on this kind of surfaces. Unfortunately, the quality of these films is usually not very high and/or the deposition process has a significant negative effect on properties of graphene. Thus, in order to cover graphene with uniform high-quality dielectric layers, different approaches to initiate the film growth have been investigated. It has been demonstrated that a seed layer can be grown by ALD on graphene using highly reactive precursors and very low deposition temperatures close to room temperature. Another way is to functionalize the graphene surface by deposition of metal or polymer buffer layers. It has to be noted, however, that functionalization, for instance with a metal seed layer can lead to degradation of the electronic properties of graphene. On the other hand, in the case of polymeric buffer layers, even when the electronic properties of graphene are not affected much, the total thickness of polymer/high-k dielectric layer might be too big for some kind of applications. Thus, the processes for deposition of dielectrics on graphene definitely need further optimization. It should also be pointed out that only a limited number of ALD experiments have been performed on CVD graphene, which has a great potential as a material for future nanoelectronics.

5. Acknowledgment

We would like to thank Pertti Hakonen for supporting the initiation of graphene studies at the Institute of Physics of the University of Tartu, Kaupo Kukli for useful discussions and Aleks Aidla and Alma-Asta Kiisler for technical assistance in experiments. This work was supported by Estonian Science Foundation (Grants No. 6651, 6999, 7845 and 8666), Estonian Ministry of Education and Research (targeted project SF0180046s07) and European Social Fund (Grant MTT1).

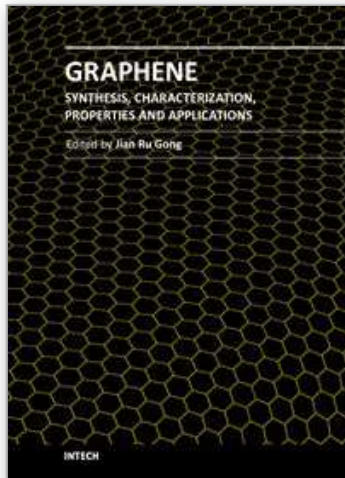
6. References

- Alles, H.; Aarik, J.; Aidla, A.; Fay, A.; Kozlova, J.; Niilisk, A.; Pärs, M.; Rähn, M.; Wiesner, M.; Hakonen, P. & Sammelselg, V. (2011). Atomic Layer Deposition of HfO₂ on Graphene from HfCl₄ and H₂O. *Central European Journal of Physics* 9(2): 319-324
- Bae, S.; Kim, H.; Lee, Y.; Xu, X.; Park, J.-S.; Zheng, Y.; Balakrishnan, J.; Lei, T.; Kim, H.R.; Song, Y.I.; Kim, Y.J.; Kim, K.S.; Özyilmaz, B.; Ahn, J.-H.; Hong, B.H. & Iijima, S. (2010). Roll-to-Roll Production of 30-inch Graphene Films for Transparent Electrodes. *Nature Nanotechnology* 5(8): 574-578
- Bao, W.; Miao, F.; Chen, Z.; Zhang, H.; Jang, W.; Dames, C. & Lau, C.N. (2009). Controlled Ripple Texturing of Suspended Graphene and Ultrathin Graphite Membranes. *Nature Nanotechnology* 4(9): 562-566
- Bolotin, K.I.; Sikes, K.J.; Hone, J.; Stormer, H.L. & Kim, P. (2008). Temperature-Dependent Transport in Suspended Graphene. *Physical Review Letters* 101(9): 096802
- Casiraghi, C.; Pisana, S.; Novoselov, K.S.; Geim, A.K. & Ferrari A.C. (2007). Raman Fingerprint of Charged Impurities in Graphene. *Applied Physics Letters* 91(23): 233108
- Das, A.; Pisana, S.; Chakraborty, B.; Piscanec, S.; Saha, S.K.; Waghmare, U.V.; Novoselov, K.S.; Krishnamurthy, H.R.; Geim, A.K.; Ferrari, A.C. & Sood, A.K. (2008). Monitoring Dopants by Raman Scattering in an Electrochemically Top-Gated Graphene Transistor. *Nature Nanotechnology* 3(4): 210-215
- Fallahazad, B.; Kim, S.; Colombo, L. & Tutuc, E. (2010). Dielectric Thickness Dependence of Carrier Mobility in Graphene with HfO₂ Top Dielectric. *Applied Physics Letters* 97(12): 123105
- Farmer, D.B. & Gordon R.G. (2006). Atomic Layer Deposition on Suspended Single-Walled Carbon Nanotubes via Gas-Phase Noncovalent Functionalization. *Nano Letters*, 6(4): 699-703
- Farmer, D.B.; Chiu H.-Y.; Lin Y.-M.; Jenkins, K.A.; Xia, F. & Avouris P. (2009). Utilization of a Buffered Dielectric to Achieve High Field-Effect Carrier Mobility in Graphene Transistors. *Nano Letters*, 9(12): 4474-4478
- Hesjedal, T. (2011) Continuous Roll-to-Roll Growth of Graphene Films by Chemical Vapor Deposition. *Applied Physics Letters* 98(13): 133106
- Kim, S.; Nah, J.; Jo, I.; Shahrjerdi, D.; Colombo, L.; Yao, Z.; Tutuc, E. & Banerjee, S.K. (2009). Realization of a High Mobility Dual-Gated Graphene Field-Effect Transistor with Al₂O₃ Dielectric. *Applied Physics Letters* 94(6): 062107
- Lee, B.; Park, S.-Y.; Kim, H.-C.; Cho, K.J.; Vogel, E.M.; Kim, M.J.; Wallace, R.M. & Kim J. (2008). Conformal Al₂O₃ Dielectric Layer Deposited by Atomic Layer Deposition for Graphene-Based Nanoelectronics. *Applied Physics Letters* 92(20): 203102
- Lee, B.; Mordi, G.; Kim, M.J.; Chabal, Y.J.; Vogel, R.M.; Wallace, R.M., Cho, K.J.; Colombo, L. & Kim, J. (2010). Characteristics of High-k Al₂O₃ Dielectric Using Ozone-Based Atomic Layer Deposition for Dual-Gated Graphene Devices. *Applied Physics Letters* 97(4): 043107
- Lemme, M.C.; Echtermeyer, T.J; Baus, M. & Kurz, H. (2007). A Graphene Field-Effect Device, *IEEE Electron Device Letters* 28(4): 282-284

- Lin, Y.-M.; Dimitrakopoulos, C.; Jenkins, K.A.; Farmer, D.B.; Chiu, H.-Y.; Grill, A. & Avouris, P. (2010). 100-GHz Transistors from Wafer-Scale Epitaxial Graphene. *Science* 327:662
- Lin, Y.-M.; Jenkins, K.A.; Valdes-Garcia, A.; Small, J.P.; Farmer, D.B. & Avouris, P. (2009). Operation of Graphene Transistors at Gigahertz Frequencies. *Nano Letters* 9(1): 422-426
- Meric, I.; Han, M.Y.; Young, A.F.; Özyilmaz, B.; Kim, P. & Shepard, K.L. (2008). Current Saturation in Zero-Bandgap, Top-Gated Graphene Field-Effect Transistors. *Nature Nanotechnology* 3(11): 654-659
- Meric, I.; Dean, C.R.; Young, A.F.; Baklitskaya, N.; Tremblay, N.J.; Nuckolls, C.; Kim, P. & Shepard, K.L. (2011). Channel Length Scaling in Graphene Field-Effect Transistors Studied with Pulsed Current-Voltage Measurements. *Nano Letters* 11(3): 1093-1097
- Mohiuddin, T.M.G; Lombardo, A.; Nair, R.R.; Bonetti, A.; Savini, G.; Jalil, R.; Bonini, N.; Basko, D.M.; Galiotis, C.; Marzari, N.; Novoselov, K.S.; Geim, A.K. & Ferrari, A.C. (2009). Uniaxial Strain in Graphene by Raman Spectroscopy: G Peak Splitting, Grüneisen Parameters, and Sample Orientation. *Physical Review B* 79(20): 205433
- Moon, J.S.; Curtis, D.; Hu, M.; Wong, D.; McGuire, C.; Campbell, P.M.; Jernigan, G.; Tedesco, J.L.; VanMil, B.; Myers-Ward, R.; Eddy, C, Jr.; Gaskill, D.K. (2009). Epitaxial-Graphene RF Field-Effect Transistors on Si-Face 6H-SiC Substrates. *IEEE Electron Device Letters* 30(6): 650-652
- Nayfeh, O.M.; Marr, T. & Dubey, M. (2011). Impact of Plasma-Assisted Atomic-Layer-Deposited Gate Dielectric on Graphene Transistors. *IEEE Electron Device Letters* 32(4): 473-475
- Ni, Z.H.; Wang, H.M.; Ma, Y.; Kasim, J; Wu, Y.H. & Shen, Z.X. (2008a). Tunable Stress and Controlled Thickness Modification in Graphene by Annealing. *ACS Nano* 2(5): 1033-1039
- Ni, Z.H.; Wang, Y.; Yu, T. & Shen, Z. (2008b). Raman Spectroscopy and Imaging of Graphene. *Nano Research* 1(4): 273-291.
- Novoselov, K.S.; Geim, A.K.; Morozov, S.V.; Jiang, D.; Zhang, Y.; Dubonos, S.V.; Grigorieva, I.V. & Firsov, A.A. (2004). Electric Field Effect in Atomically Thin Carbon Films. *Nature* 306 : 666-669
- Robinson, J.A.; Ill, M.L.; Trumbull, K.A.; Weng, X.; Cavelero, R.; Daniels, T.; Hughes, Z.; Hollander, M.; Fanton, M. & Snyder, D. (2010). Epitaxial Graphene Materials Integration: Effects of Dielectric Overlayers on Structural and Electronic Properties. *ACS Nano* 4(5): 2667-2672
- Wang, J.; Li, H.P. & Stevens, R. (1992). Hafnia and Hafnia-Toughened Ceramics. *Journal of Materials Science* 27(20): 5397-5430
- Wang, X.; Tabakman, S.M. & Dai, H. (2008). Atomic Layer Deposition of Metal Oxides on Pristine and Functionalized Graphene. (2008). *Journal of American Chemical Society* 130(26): 8152-8153
- Williams, J.R.; DiCarlo, L. & Marcus, C.M. (2007). Quantum Hall Effect in a Gate-Controlled p-n Junction of Graphene. *Science* 317: 638-641

- Wu, Y.; Lin, Y.-M.; Bol, A.A.; Jenkins, K.A.; Xia, F.; Farmer, D.B.; Zhu, Y. & Avouris, P. (2011). High-Frequency, Scaled Graphene Transistors on Diamond-like Carbon. *Nature* 472: 74-78
- Xuan, Y.; Wu, Y.Q.; Shen, T.; Qi, M.; Capano, M.A.; Cooper, J.A. & Ye, P.D. (2008). Atomic-Layer-Deposited Nanostructures for Graphene-Based Nanoelectronics. *Applied Physics Letters* 92(1): 013101
- Zou, K.; Hong, X.; Keefer, D. & Zhu, J. (2010). Deposition of High-Quality HfO₂ on Graphene and the Effect of Remote Oxide Phonon Scattering. *Physical Review Letters*, 105(12): 126601

IntechOpen



Graphene - Synthesis, Characterization, Properties and Applications

Edited by Prof. Jian Gong

ISBN 978-953-307-292-0

Hard cover, 184 pages

Publisher InTech

Published online 15, September, 2011

Published in print edition September, 2011

The discovery of graphene has led to a deluge of international research interest, and this new material in the field of materials science and condensed-matter physics has revealed a cornucopia of new physics and potential applications. This collection gives a roughly review on the recent progress on the synthesis, characterization, properties and applications of graphene, providing useful information for researchers interested in this area.

How to reference

In order to correctly reference this scholarly work, feel free to copy and paste the following:

Harry Alles, Jaan Aarik, Jekaterina Kozlova, Ahti Niilisk, Raul Rammula and Väino Sammelselg (2011). Atomic Layer Deposition of High-k Oxides on Graphene, Graphene - Synthesis, Characterization, Properties and Applications, Prof. Jian Gong (Ed.), ISBN: 978-953-307-292-0, InTech, Available from: <http://www.intechopen.com/books/graphene-synthesis-characterization-properties-and-applications/atomic-layer-deposition-of-high-k-oxides-on-graphene>

INTECH
open science | open minds

InTech Europe

University Campus STeP Ri
Slavka Krautzeka 83/A
51000 Rijeka, Croatia
Phone: +385 (51) 770 447
Fax: +385 (51) 686 166
www.intechopen.com

InTech China

Unit 405, Office Block, Hotel Equatorial Shanghai
No.65, Yan An Road (West), Shanghai, 200040, China
中国上海市延安西路65号上海国际贵都大饭店办公楼405单元
Phone: +86-21-62489820
Fax: +86-21-62489821

© 2011 The Author(s). Licensee IntechOpen. This chapter is distributed under the terms of the [Creative Commons Attribution-NonCommercial-ShareAlike-3.0 License](#), which permits use, distribution and reproduction for non-commercial purposes, provided the original is properly cited and derivative works building on this content are distributed under the same license.

IntechOpen

IntechOpen